X-646-72-151
PREPRINT

NASA TM X- 65902

PRECIPITATION OF LOW-ENERGY ELECTRONS AT HIGH LATITUDES: EFFECTS OF SUBSTORMS, INTERPLANETARY MAGNETIC FIELD AND DIPOLE TILT ANGLE

J. L. BURCH

MAY 1972

GSFC — GODDARD SPACE FLIGHT CENTER
GREENBELT, MARYLAND

PRECIPITATION OF LOW-ENERGY ELECTRONS AT HIGH LATITUDES: EFFECTS OF SUBSTORMS, INTERPLANETARY MAGNETIC FIELD AND DIPOLE TILT ANGLE

By

J. L. Burch
NASA-Goddard Space Flight Center
Greenbelt, Maryland 20771

MAY 1972

ABSTRACT

Data from the Auroral Particles Experiment on OGO-4 were used to study effects of substorm activity, interplanetary magnetic field latitude and dipole tilt angle on high-latitude precipitation of 700 ev electrons. It was found that: (1) The high-latitude zone of 700 ev electron precipitation in late evening and early morning hours moves equatorward by 5-10° during substorms. This behavior is interpreted as an effect of the substorm-associated thinning of the plasma sheet. (2) The low-latitude boundary of polar cusp electron precipitation at 9-15 hours MLT also moves equatorward by several degrees during substorms and, in the absence of significant substorm activity, after a period of southward interplanetary magnetic field. This behavior is interpreted to result from erosion of dayside magnetic flux into the tail and to be a part of the substorm growth phase. Flux conservation calculations indicate that the observations are consistent with a model of dayside flux erosion by a southward interplanetary magnetic field provided the magnetopause is roughly 20-30% transparent to external fields. (3) With times containing substorm activity or a southward interplanetary magnetic field eliminated, the low-latitude boundary of polar cusp electron precipitation is found to move by approximately 4° over the total yearly range of tilt angles. At maximum winter and summer conditions the invariant latitude of the boundary is shown to shift by approximately -3° and +1° respectively from its equinox location. This same asymmetry is found in calculations of the invariant latitude of the first open field line in the Mead-Fairfield model magnetosphere. The observed polar cusp lower boundaries lie approximately 3° below the calculated first open field lines and coincide with the average > 35 kev electron boundaries of Feldstein and Starkov.

INTRODUCTION

The morphology of high-latitude electron precipitation has been studied extensively by several groups over the past decade. See Hoffman (1971) and Paulikas (1971) for recent comprehensive reviews. Dating from the initial finding (see Johnson et al, 1966; Sharp and Johnson, 1968; Johnson and Sharp, 1969) that the dayside precipitation zone is divided into a well-defined hard zone and a higher latitude soft zone, further observations have confirmed that a soft zone is generally present at all local times, although the division is much more distinct on the day side than on the night side, where substorm effects often change its character significantly.

The intense, highly variable, and sometimes field-aligned (see Hoffman and Evans, 1968) electron fluxes present in the soft zone have been identified either causally or spatially with several high-latitude geophysical phenomena, including discrete auroral forms (Hoffman and Berko, 1971), VLF hiss (Gurnett and Frank, 1972; Hoffman and Laaspere, 1972), 6300 Å emissions (Sandford, 1970; Evans et al, 1972), and possibly the winter polar ionosphere (Maehlum, 1968; Burch, 1970; Pike, 1971). Recently Heikkila and Winningham (1971) have found evidence that the dayside soft zone is produced by penetration of thermalized solar wind through the magnetospheric neutral lines or polar cusps. This evidence was based on a comparison of electron and proton spectra in the magnetosheath and in the low-altitude soft zone. Frank (1971b) has measured electron and proton spectra and pitch-angle distributions in the mid-altitude polar cusp ($R \sim 5\ R_E$). Frank also found good agreement between polar cusp and magnetosheath particle spectra, and further noted a

separation between the electron and proton zones with the proton precipitation lying just poleward of the electron precipitation. Both Heikkila and Winningham (1971) and Frank (1971b) concluded that the zone lies just poleward of the high-latitude limit of closed field lines and the > 40 kev electron trapping boundary.

Based on comparison of particle spectra (e.g., by Burch, 1968a, and Hones, et al, 1971) and on determination of the relationship of the > 40 kev electron trapping boundary and the plasma sheet by Frank (1971a) the nightside soft zone has been interpreted as the low-altitude extension of the plasma sheet. During periods of substorm activity the intense fluxes of low-energy electrons in the nightside soft zone are often accompanied by large fluxes of electrons of several kev energy (Burch, 1970; Hoffman, 1972). Near dawn and dusk the division, if any, between the polar cusp and the plasma sheet has not been determined.

That the location of the high-latitude soft zone is a strong function of magnetic local time and magnetic activity has been known for some time (see, Burch, 1968b, 1970; Hoffman, 1971; Hoffman and Berko, 1971). Maehlum (1968) has also noted an apparently large dipole-tilt-angle dependence of the high-latitude boundary of low-energy precipitation near noon and midnight.

The purpose of this study is to examine the movement in latitude of low-energy electron precipitation in response to substorm activity and a southward-turning interplanetary magnetic field. With these effects eliminated, the tilt angle dependence of the location of the dayside soft zone, or polar cusp, is reevaluated and found to be somewhat

weaker than previously found by Maehlum (1968) and inferred from Feldstein and Starkov (1970).

EXPERIMENTAL DETAILS

Electron data from the OGO-4 Auroral Particles Experiment (Hoffman and Evans, 1967) are used in this study. The experiment consisted of seven cylindrical electrostatic analyzers which measured directional fluxes of 0.7, 2.3, 7.3 and 23.9 kev electrons arriving along the earth's radius vector and fluxes of 2.3 kev electrons at 30^{o}, 60^{o} and 90^{o} to the radius vector. In high-latitude regions, where $\bar{B}$ is nearly radial at the nominal OGO-4 altitude of 700 km, the 0^{o} detectors measured precipitated electrons. Only the 0.7 and 7.3 kev detectors are discussed herein.

SUBSTORM EFFECTS

As mentioned above, it has been found previously that the regions of particle precipitation move to lower latitudes when K_p increases. However, during this study it has been found that K_p and the available AE values are not sufficient to predict the approximate location of the zone of precipitation. The phase of individual substorms and the latitude of the interplanetary magnetic field have been found to be of more importance, with large changes in the latitude of precipitation resulting even during periods of very low K_p and AE. An example of the lowering of the high-latitude boundary of 0.7 kev electron precipitation during substorm activity is shown in Figure 1. 2.5-minute AE values are plotted along the vertical axis. K_p values for the five passes shown

were 2^+, 2^+, 3, 3, and 3^-. Approximate invariant latitudes are shown across the top of the figure, the actual horizontal axis being in units of universal time. In each case the high-latitude boundary of precipitation (excluding isolated narrow spikes) is located exactly on the invariant latitude axis, with the discrepancy at other times being in no case more than one degree. These passes crossed the polar cap from the morning side to the evening side. During quiet times (as indicated by the AE values) 700 ev electrons extended to or above $\Lambda = 80^\circ$. During the period of increased substorm activity, in the 4th pass, the zone of precipitation moved nearly 10° equatorward in both early morning and evening hours. Several hours later, when the activity had terminated, the regions of precipitation had again moved poleward. The last pass was actually on the day side in magnetic local time, crossing from 9.4 hours to 14 hours. The morning portion of this pass is typical of day-side crossings during quiet times, with a sharp low-latitude boundary of precipitation which we identify as the lower boundary of the polar cusp. A data gap occurred before the satellite crossed the low-latitude polar cusp boundary in the afternoon sector. Typically, except for isolated spikes, all higher energy channels are below threshold in the polar cusp, in agreement with the spectra found by Heikkila and Winningham (1971). As in the last pass in Figure 1, the polar cusp is generally found to be $3\text{-}5^\circ$ wide, as concluded by Heikkila and Winningham.

Unambiguous determination of the low-latitude boundary of polar cusp precipitation is nearly always possible because of its sharp onset and the fact that OGO-4 generally reached invariant latitudes well above

the lower boundary. On the other hand, the upper boundary is typically harder to identify because of the frequent existence of localized spikes or drizzle of precipitation into the polar cap (see also Heikkila and Winningham, 1972) and because OGO-4 (as all other low-altitude polar-orbiting satellites) frequently did not reach high enough invariant latitudes to pass out of the polar cusp and far enough into the polar cap to provide an unambiguous boundary location. For this reason the study of the polar cusp location which follows is based primarily on its low-latitude boundary.

An example of the equatorward movement of the low-latitude boundary of the polar cusp is shown in Figure 2. This pass began during the period between two substorms with the breakup of the second storm occurring as OGO-4 crossed from the morning side to the afternoon side. The low-latitude boundary of the polar cusp precipitation was significantly below typical quiescent locations (see Figure 1) during this crossing, which occurred either just before or very near the breakup of the second substorm. Data from the Ames magnetometer experiment on Explorer 33 (located near 19.5 hours local time in the magnetosheath) indicate that the interplanetary magnetic field had a southward component of 2-3γ during this period. It thus appears that the anomalously low boundary location was either a residual effect of the first substorm or was associated with the southward interplanetary magnetic field and the growth phase of the second substorm. This question is considered further in the next section.

EFFECTS OF INTERPLANETARY MAGNETIC FIELD LATITUDE

After eliminating times when significant substorm activity was present, there were still many cases of anomalously low polar cusp lower boundaries. Preceding every such case was a significant period of southward interplanetary magnetic field ($\bar{B}_{IMF}$). An example of this behavior is shown in Figure 3. The $\bar{B}_{IMF}$ z component in geocentric solar magnetospheric (GSM) coordinates is plotted in the upper panel. Three passes of OGO-4 are shown in the lower plots. All three passes were at geographic local times of 8-12 hours. The first pass occurred after a large substorm when the interplanetary field was nearly horizontal. The magnetic local time of this pass is actually 05 hours, so its identification with the polar cusp is questionable. However, the location of the lower boundary of precipitation and its general character are consistent with what is seen in later morning hours when $\bar{B}_{IMF}$ is northward. The second pass occurred after a considerable period of southward $\bar{B}_{IMF}$. However, as indicated by the low AE hourly values listed, no significant substorm activity resulted, perhaps because the total period of southward field was only about one hour (see Foster et al, 1971). Magnetograms from this period are shown in Figure 4. Although several stations were in the midnight sector, only Churchill showed any significant electrojet activity during this first period of southward field. The Churchill negative activity was accompanied by large negative Z deviations, indicating a current well to the north of Churchill (Λ = 70.1°). In any case, the relatively weak activity at Churchill had almost completely recovered by the time of the OGO-4 polar cusp boundary crossing (0650 UT). The third pass located the polar cusp boundary at

$\Lambda = 78.4^{o}$, or its approximate quiescent position. This pass occurred only about 9 minutes after the onset of the southward $\bar{B}_{IMF}$ at the earth. The magnetograms in Figure 4 show no auroral zone activity during this period of southward $\bar{B}_{IMF}$.

The time that the southward interplanetary magnetic field actually reached the earth was determined in both cases by examination of polar-cap and equatorial magnetograms in conjunction with data from the Ames magnetometer experiment on Explorers 33 and 35. As discussed by Nishida and Kokubun (1971) and Burch (1972), a southward-turning $\bar{B}_{IMF}$ produces a near simultaneous response in the polar cap and at the equator while significant auroral zone substorm activity follows by one hour or more (see Arnoldy, 1971; Foster et al, 1971). In all cases discussed below, the arrival time of southward $\bar{B}_{IMF}$ is determined by identifying the onset time of the associated ground magnetic disturbances at several polar cap and equatorial stations. In Figure 4 are shown the polar cap and equatorial disturbances associated with the two periods of southward $\bar{B}_{IMF}$ discussed in connection with Figure 3. In each case the sudden onset of southward magnetic field produced a noticeable disturbance at Thule. The southward excursion at 0545 UT also produced a fairly large disturbance at Annamalainagar ($L < 1$) and noticeable transient disturbances at Barrow, College and Sitka. In each case the duration of the disturbance at Thule is within a few minutes of the duration of the increased southward $\bar{B}_{IMF}$ at Explorer 35. This fact and the absence of large polar cap disturbances preceding the onset of the southward field makes an unambiguous identification of the resulting polar cap disturbance possible in this and similar cases. However, during disturbed times this

method is often not feasible and other less accurate methods of timing are necessary (see Fairfield, 1967; Aubry and McPherron, 1971). Of course, if magnetic field measurements are available in the dayside magnetosheath or from two satellites which are near the earth-sun line, accurate determinations of the arrival time of $\bar{B}_{IMF}$ discontinuities are possible even during highly disturbed times. The onset times determined in this study are accurate to within approximately $\pm$ 4 minutes. However, movement of the polar cusp lower boundary may begin a few minutes before any effects are noted on the ground. Errors resulting from such a time delay will be approximately equal for all cases considered below.

Examination of the total 1½ years of OGO-4 data resulted in 10 clear-cut cases when the interplanetary magnetic field turned sharply and appreciably southward and a polar cusp crossing occurred between 09-15 hours MLT. The magnitude of the southward component of $\bar{B}_{IMF}$ for these cases was in the range 1.5-5γ in solar equatorial (GSEQ) coordinates and 1-6.8γ in solar magnetospheric (GSM) coordinates. The average GSM southward component for the 10 cases was 3.0γ. In each case it was required that the sharp onset of southward $\bar{B}_{IMF}$ was preceded by at least a half hour of nearly horizontal or northward $\bar{B}_{IMF}$ during which relatively quiet magnetic conditions prevailed. That is, while most cases of southward-turning $\bar{B}_{IMF}$ were preceded by no substorm activity, a few (as in Figure 2) occurred in the late recovery phase of substorms when nearly quiescent conditions are expected. In Figure 5 the invariant latitude of the lower boundary of polar cusp precipitation is plotted versus time after the onset of southward $\bar{B}_{IMF}$ at the earth, determined

as described above. The data in Figures 2 and 3 are included. Some scatter is expected (at least near zero time) due to differences in dipole tilt angle. Based on the discussion below, the maximum scatter is estimated to be 2.5^{o} over the limited range of tilt angles (75.6^{o} - 114.7^{o}) included. It is evident from Figure 5 that large changes in the latitude of the polar cusp lower boundary occur in conjunction with a southward component of $\bar{B}_{IMF}$. Moreover, the location of the polar cusp boundary shows a dependence on the length of time after the onset of the southward interplanetary magnetic field. For the relatively quiet times considered, all cases of anomalously low polar cusp boundaries occurred in conjunction with a southward $\bar{B}_{IMF}$, even though in many cases the transition from northward to southward $\bar{B}_{IMF}$ was not distinct enough for a reliable onset time to be determined. Such cases could not be included in Figure 5. The observations summarized in Figure 5 are interpreted as direct evidence for gradual erosion of dayside magnetic flux by the southward interplanetary field, which is often followed by a substorm expansion phase (see Figure 2).

Evidence of erosion of dayside magnetic field lines has also been found by Aubry et al (1970) before a substorm and by Russell et al (1971) and Akasofu (1972) during substorms. Aubry et al (1970) observed, in a single case, an inward motion of the magnetopause just prior to a substorm. This motion was not accompanied by magnetospheric compression and was interpreted to be part of the substorm growth phase. Russell et al (1971) have observed relative movement of the polar cusp to lower and higher latitudes as $\bar{B}_{IMF}$ turned southward and northward, respectively,

during the large magnetic storm of November 1, 1968, when $\bar{B}_{IMF}$ southward components of 25-30γ were observed. The polar cusp lower boundary was encountered at estimated invariant latitudes down to 66° during this storm. Akasofu (1972) has observed equatorward motion of midday auroras during the expansion phase of substorms and a return poleward during the subsequent recovery phases.

Although the mechanism of field line reconnection is not completely understood (see, e.g., Yeh and Axford, 1970), the data of Figure 5 provide evidence that it does occur while also providing some measure of its efficiency. To what degree the diamagnetic effects of magnetopause currents shield the magnetosphere from the interplanetary magnetic field is not known (see, e.g., Forbes and Speiser, 1971). However, reconnection of interplanetary and geomagnetic field lines requires that the shielding not be complete and that a normal component of $\bar{B}$ can exist across the magnetopause. Assuming that the quiescent position of the lower boundary of the polar cusp is at $\Lambda = 78^{\circ}$ and that this field line maps onto the dayside magnetopause, the following flux conservation calculation can be made. The magnetic field at the earth's surface is very nearly that of a dipole with a radial $\bar{B}$ component of .62 sin Λ gauss. Λ (invariant latitude) and λ (geomagnetic latitude) are, by definition, identical at $r = 1\ R_E$. Then, the magnetic flux passing through the area bounded by $\Lambda = 78^{\circ}$ on the north and $\Lambda = \Lambda_1$ on the south, and extending 0.005 radian to either side of the earth-sun line (i.e., $-.005 \leq \emptyset \leq +.005$) is given by,

$$\Phi_1 = \int_{-.005}^{.005} \int_{\Lambda_1}^{78^\circ} .62 \sin\Lambda \cos\Lambda \, d\Lambda d\phi \qquad (1)$$

$$= .0031 \left[\sin^2 (78^\circ) - \sin^2 (\Lambda_1)\right], \qquad (2)$$

with Φ_1 in units of gauss$\cdot R_E^2$. If reconnection occurs at the magnetopause near the equatorial plane, it is reasonable to expect that the portion of the composite interplanetary-geomagnetic field line lying outside the (possibly fuzzy) magnetopause (see Dungey, 1968) will be frozen into the collisionless plasma and transported with it around the flanks of the magnetosphere and into the tail region. The resulting configuration may be essentially as drawn by Dungey (1961) and Levy et al (1963) in which the interaction region at the earth's surface (that is 78° down to the first closed field line) is mapped through the magnetopause and into the interplanetary magnetic field. Flux conservation should therefore hold between the magnetic field at the surface of the earth and a certain fraction of the interplanetary magnetic field in the undisturbed solar wind which is determined by the degree of transparency of the magnetopause to the external field. Assuming that the noon-meridian magnetopause is initially located at a geocentric distance of 10 R_E in the equatorial plane, the field lines near the upper boundary ($\Lambda = 78^\circ$) of the area element described in equation (1) will map into an element of the equatorial plane of width 20 tan (.005) $\approx$ 0.1 R_E perpendicular to the earth-sun line. Assuming that this width remains constant as the field lines are transported into the tail, the field lines from the area described in equation (1) will map onto a strip of

the magnetopause of width 0.1 R_E and length determined by the solar wind velocity. With a solar wind velocity (around the magnetosphere), V_s, and an effective southward $\bar{B}_{IMF}$ (that is, after shielding by the diamagnetic magnetopause), B_{-Z}^{eff}, the following flux equality will hold,

$$\Phi_1 = \Phi_2 = 0.1\, B_{-Z}^{eff} V_s t, \qquad (3)$$

where t is the time after the onset of southward $\bar{B}_{IMF}$. Combining equations (2) and (3) and assigning values to B_{-Z}^{eff} and V_s, a relation between t and Λ_1 is obtained. The curves in Figure 5 are for V_s = 400 km/s and B_{-Z}^{eff}= 0.5γ (upper curve) and B_{-Z}^{eff}= 1γ (lower curve). The general form of the relationship between Λ_1 and t indicates that the flux conservation requirements of the reconnection model are consistent with the observations provided that the magnetopause is roughly 20-30% transparent to the interplanetary magnetic field (recall that the average southward $\bar{B}_{IMF}$ component for the points in Figure 5 was 3γ).

In the simple model discussed above it is assumed that erosion can proceed indefinitely. This cannot be the case since flux is continuously being transported to the day side. In the stable situation, with no erosion, reconnection of tail magnetic field lines occurs (although it is not known where) to permit their transport to the day side by the earth's rotation. During and after a period of erosion, a similar transport process should occur. At large antisolar distances the solar wind and interplanetary magnetic field will have returned to their undisturbed state. This could result from the formation of a neutral point at an

intermediate distance down the tail (see Dungey, 1961; Levy et al, 1963) at which disconnection of the geomagnetic and interplanetary magnetic fields occurs. Therefore, erosion produced by an element of southward $\bar{B}_{IMF}$ would persist only until the element passed beyond the tail neutral point. Depending on the distance of the neutral (or disconnection) point down the tail, a limit will be placed on the total amount of magnetic flux which can be transferred from the day side into the tail for a given B_{-Z}^{eff} and V_s. There is some evidence for such a leveling off in the data of Figure 5, although this does not show up in the calculation of equation (3).

EFFECTS OF DIPOLE TILT

Again considering magnetic local times 09 - 15 hours, the tilt-angle dependence of the lower boundary of the polar cusp has been studied after eliminating all times with substorm activity or when there was a southward interplanetary magnetic field. The results are shown in Figure 6. All data are for 09 - 15 hours MLT in the northern hemisphere, with no substorm activity apparent in 2.5-minute AE values, and a northward $\bar{B}_{IMF}$. With substorm and southward interplanetary magnetic field effects eliminated, there is a total seasonal shift of 4^o in the invariant latitude of the lower boundary of polar cusp electron precipitation. Approximately 3^o of this shift occurs for β (tilt angle) $> 90^o$ (northern winter conditions) with only a 1^o shift for $\beta < 90^o$. Therefore, the maximum universal time dependence over a single day will occur at the winter solstice, amounting to only 2.5^o.

Also shown in Figure 6 are the results of calculations of the location of the first open field line using the model of Mead and Fairfield (1971). The calculations were made as follows. Noon meridian field lines were traced from the surface of the earth outward in the northern hemisphere. If, as the field line was traced outward the condition, $B_x > 0$, $B_z < 0$ in solar magnetic coordinates, was found, the field line was labeled "open". If the condition, $B_x < 0$, $B_z > 0$, was found, the field line was labeled "closed". Latitude increments of 0.1^o were used, so for this calculation there was at most a 0.1^o difference between the latitudes of the first open field line and the last closed field line. In this model, as in the various mathematical models, tracing of field lines which pass very near the neutral points will often lead to lost field lines which never return to the earth. Therefore, although the field line 0.1^o below the first open field line plotted in Figure 6 is not swept back into the tail in the Mead-Fairfield model, it does not necessarily connect directly to the southern hemisphere. The first open field lines calculated are to be viewed as those which pass very near the average magnetospheric neutral points for $K_p \leq 2$ in the Mead-Fairfield model. In Figure 6, the observed lower boundaries are clustered about a curve lying 3^o below the calculated first open field lines. This is roughly consistent with the $3\text{-}5^o$ observed width of the polar cusp precipitation. Also plotted are the average locations of the last closed field line in the local time sector 10-18 hours as observed by Feldstein and Starkov (1970). The last closed field line in their study was interpreted to be coincident with the boundary where > 35 kev electron fluxes dropped to cosmic-ray

background. Since the > 35 kev electron trapping boundary lies at or near the low-latitude boundary of polar cusp precipitation (see Heikkila and Winningham, 1971; Frank, 1971b), the two boundaries are expected to show similar behaviors with changing tilt angle. As shown in Figure 6, good agreement is found over the limited range of tilt angles covered by Feldstein and Starkov's study. However, a linear extrapolation of their points would predict a much stronger tilt-angle dependence than is found here. Feldstein and Starkov's data covered times when the magnetic activity index Q was less than 3 (somewhat quieter than $K_p < 3$) so, while some scatter would be expected due to substorm activity and southward $\bar{B}_{IMF}$, the effect on their average boundary locations is expected to be minimized to a degree.

Maehlum (1968) has studied the high-latitude boundary of precipitation of > 50 ev electrons near noon and midnight. This boundary on the day side coincides with the high-latitude edge of polar cusp precipitation. Restricting his study only to $K_p \leq 4$, Maehlum found nearly a 10^o variation over the total range of tilt angles. Hoffman (1971), noting a K_p dependence for $K_p \leq 4$ which was greater than the UT dependence for $K_p \leq 1+$, restricted both his measurements and those of Maehlum (1968) to $K_p \leq 1+$, and found only about a $2\frac{1}{2}^o$ change in the high-latitude boundary of precipitation. Again, effects of southward $\bar{B}_{IMF}$ and isolated substorms were not eliminated. In Figure 7, Hoffman's (1971) Figure 12 is reproduced with the following modifications: (1) cases where $\bar{B}_{IMF}$ was clearly southward and/or when a substorm was in progress (as deduced from 2.5-minute AE values) are indicated by solid circles, (2) cases

when there was no substorm activity but $\bar{B}_{IMF}$ was very nearly horizontal and was neither clearly northward nor southward are plotted with squares. Open circles are cases with no substorm activity and $\bar{B}_{IMF}$ clearly northward. Elimination of all solid points from Figure 7 would result in about a 4^{o} tilt-angle dependence in agreement with that shown in Figure 6 for the low-latitude boundary.

SUMMARY

The high-latitude zone of low-energy electron precipitation in late evening and early morning hours is shown to move equatorward by several degrees during substorms. This behavior is interpreted as resulting from the substorm-associated thinning of the plasma sheet which has been reported by Aubry and McPherron (1971) and others. Similar behavior is noted on the dayside, where the low-latitude boundary of polar cusp electron precipitation is found at much lower latitudes than its quiescent position even during weak substorm activity. Furthermore, anomalously low polar cusp latitudes are often observed before substorm breakups and in the absence of significant substorm activity. All such cases occurred during periods when the interplanetary magnetic field at the earth had a southward component in solar magnetospheric coordinates. It is concluded that the equatorward movement of the polar cusp occurs prior to the substorm breakup and is part of the substorm growth phase. Support is therefore given to the observation by Aubry et al (1970) of the inward motion of the magnetopause prior to a substorm.

Analysis of 10 polar cusp crossings which followed sharp onsets of southward $\bar{B}_{IMF}$ shows that the latitude of the polar cusp lower boundary moves gradually equatorward at an approximate rate of .1°/ min. for GSM southward magnetic field components averaging 3γ. A flux conservation calculation indicates that this dependence is consistent with a model of flux erosion from the dayside and into the tail provided that the magnetopause is roughly 20-30% transparent to external fields.

With times containing substorm activity or a southward $\bar{B}_{IMF}$ eliminated, the low-latitude boundary of the polar cusp is found to move by approximately 4° over the total yearly range of tilt angles. At maximum winter and summer conditions the low-latitude polar cusp boundary is found to shift by approximately -3° and +1° respectively from its equinox location. This same asymmetry is found in calculations of the location of the first open field line from the model of Mead and Fairfield (1971). The observed polar cusp lower boundaries are found to lie approximately 3° below the boundaries calculated from the Mead-Fairfield model and to coincide with the average last closed field line, or > 35 kev electron boundary of Feldstein and Starkov (1970). When periods with substorms and southward $\bar{B}_{IMF}$ are eliminated, the tilt-angle dependence of the upper boundary of the polar cusp found by Maehlum (1968) (10°) and Hoffman (1971) (2½°) is shown to be more nearly in agreement with that found here for the low-latitude boundary.

ACKNOWLEDGMENT

AE values and data from the Ames Magnetic Field Experiment on Explorers 33 and 35 were provided by the National Space Science Data Center. I am grateful to Dr. R. Hoffman for providing access to data from the OGO-4 Auroral Particles Experiment and for helpful discussions; to Mr. F. Berko for extensive information on the OGO-4 data reduction programs and for helpful discussions; and to Mr. R. Janetzke for significant programming assistance.

REFERENCES

Akasofu, S.-I., Midday auroras at the south pole during magnetospheric substorms, J. Geophys. Res., 77, 2303, 1972.

Arnoldy, R. L., Signature in the interplanetary medium for substorms, J. Geophys. Res., 76, 5189, 1971.

Aubry, M. P., and R. L. McPherron, Magnetotail changes in relation to the solar wind magnetic field and magnetospheric substorms, J. Geophys. Res., 76, 4381, 1971.

Aubry, M. P., C. T. Russell, and M. G. Kivelson, On inward motion of the magnetopause preceding a substorm, J. Geophys. Res., 75, 7018, 1970.

Burch, J. L., High-latitude satellite observations of electrons and protons at 4000 km, Ph.D. thesis, Rice University, Houston, Texas, May, 1968a.

Burch, J. L., Low-energy electron fluxes at latitudes above the auroral zone, J. Geophys. Res., 73, 3585, 1968b.

Burch, J. L., Satellite measurements of low energy electrons precipitated at high latitudes, in The Polar Ionosphere and Magnetospheric Processes, ed. by G. Skovli, Gordon and Breach, New York, 1970.

Burch, J. L., Effects of interplanetary magnetic field azimuth on auroral zone and polar cap magnetic activity, NASA-Goddard Space Flight Center Preprint, X646-72-115, April, 1972.

Dungey, J. W., Interplanetary magnetic field and auroral zones, Phys. Rev. Letters, 6, 47, 1961.

Dungey, J. W., The reconnection model of the magnetosphere, in Earth's Particles and Fields, ed. by B. M. McCormac, Reinhold, New York, 1968.

Evans, D. S., T. Jacobsen, B. N. Maehlum, G. Skovli and T. Wedde, Low energy electron precipitation and the ionospheric F-region in and north of the auroral zone, Planet. Space Sci., 20, 233, 1972.

Fairfield, D. H., The ordered magnetic field of the magnetosheath, J. Geophys. Res., 72, 5865, 1967.

Feldstein, Y. I., and G. V. Starkov, The auroral oval and the boundary of closed field lines of geomagnetic field, Planet. Space Sci., 18, 501, 1970.

Forbes, T. G., and T. W. Speiser, Mathematical models of the open magnetosphere: Application to dayside auroras, J. Geophys. Res., 76, 7542, 1971.

Foster, J. C., D. H. Fairfield, K. W. Ogilvie, and T. J. Rosenberg, Relationship of interplanetary parameters and occurrence of magnetospheric substorms, J. Geophys. Res., 76, 6971, 1971.

Frank, L. A., Relationship of the plasma sheet, ring current, trapping boundary, and plasmapause near the magnetic equator and local midnight, J. Geophys. Res., 76, 2265, 1971a.

Frank, L. A., Plasma in the earth's polar magnetosphere, J. Geophys. Res., 76, 5202, 1971b.

Gurnett, D. A., and L. A. Frank, VLF hiss and related plasma observations in the polar magnetosphere, J. Geophys. Res., 77, 172, 1972.

Heikkila, W. J., and J. D. Winningham, Penetration of magnetosheath plasma to low altitudes through the dayside magnetospheric cusps, J. Geophys. Res., 76, 883, 1971.

Heikkila, W. J., and J. D. Winningham, Polar cap auroral particle fluxes, EOS, Trans. AGU, 53, 501, 1972.

Hoffman, R. A., Properties of low energy particle impacts in the polar domain in the dawn and dayside hours, To be published in the proceedings of the Magnetosphere-Ionosphere Interactions Advanced Study Institute, Elsater, Norway, April 15-22, 1971.

Hoffman, R. A., Electron precipitation patterns and substorm morphology, EOS, Trans. AGU, 53, 360, 1972.

Hoffman, R. A., and F. W. Berko, Primary electron influx to dayside auroral oval, J. Geophys. Res., 76, 2967, 1971.

Hoffman, R. A., and D. S. Evans, OGO-4 auroral particles experiment and calibration, NASA-Goddard Space Flight Center preprint, X-611-671-632, 1967.

Hoffman, R. A., and D. S. Evans, Field-aligned electron bursts at high latitudes observed by OGO-4, J. Geophys. Res., 73, 6201, 1968.

Hoffman, R. A., and T. Laaspere, Comparison of very-low-frequency auroral hiss with precipitating low-energy electrons by the use of simultaneous data from two OGO-4 experiments, J. Geophys. Res., 77, 640, 1972.

Hones, E. W., Jr., J. R. Asbridge, S. J. Bame, and S. Singer, Energy spectra and angular distributions of particles in the plasma sheet and their comparison with rocket measurements over the auroral zone, J. Geophys. Res., 76, 63, 1971.

Johnson, R. G., and R. D. Sharp, Satellite measurements on auroral particle fluxes, in Atmospheric Emissions, ed. by B. M. McCormac, Reinhold, New York, 1969.

Johnson, R. G., R. D. Sharp, M. F. Shea, and G.B. Shook, Satellite observations of two distinct dayside zones of auroral electron precipitations (abstract), Trans. Am. Geophys. Union, 47, 64, 1966.

Levy, R. H., H. E. Petschek, and G. L. Siscoe, Aerodynamic aspects of magnetospheric flow, AIAA J., 2, 2065, 1963.

Maehlum, B. N., Universal-time control of the low-energy electron fluxes in the polar regions, J. Geophys. Res., 73, 3459, 1968.

Mead, G. D., and D. H. Fairfield, Quantitative magnetospheric models derived from Explorer 33, IMP 4, and IMP 5 magnetometer data, paper presented at XV General Assembly of IUGG, Moscow, August, 1971.

Nishida, A., and S. Kokubun, New polar magnetic disturbances: S_q^p, SP, DPC, and DP2, Rev. Geophys. and Space Phys., 9, 417, 1971.

Paulikas, G. A., The patterns and sources of high-latitude particle precipitation, Rev. Geophys. and Space Phys., 9, 659, 1971.

Pike, C. P., A comparison of the north - and south - polar F layers, J. Geophys. Res., 76, 6875, 1971.

Russell, C. T., C. R. Chappell, M. D. Montgomery, M. Neugebauer, and F. L. Scarf, OGO 5 observations of the polar cusp on November 1, 1968, J. Geophys. Res., 76, 6743, 1971.

Sandford, B. P., Optical emission over the polar cap, in The Polar Ionosphere and Magnetospheric Processes, ed. by G. Skovli, Gordon and Breach, New York, 1970.

Sharp, R. D., and R. G. Johnson, Satellite measurements of auroral particle precipitation, in Earth's Particles and Fields, ed. by B. M. McCormac, Reinhold, New York, 1968.

Yeh, T., and W. I. Axford, On the re-connexion of magnetic field lines in conducting fluids, J. Plasma Phys., 4, 207, 1970.

FIGURE CAPTIONS

Figure 1. A series of five passes through the polar regions from post-midnight and morning hours to afternoon and evening hours. The first four passes are on the night side and show typical patterns of precipitation of 700 ev electrons associated with the plasma sheet. The fifth pass is on the day side showing typical polar cusp electron precipitation. Arrows indicate times corresponding to the beginning of plotted data. 2.5-minute AE values are plotted along the vertical axis. K_p values for the five passes were 2+, 2+, 3, 3, and 3-. The flux scale shown for the first pass is in electrons/cm^2-ster-kev-sec. Flux thresholds are equal for all five passes.

Figure 2. An example showing the equatorward displacement of the polar cusp lower boundary associated with substorm activity and a southward interplanetary magnetic field ($\bar{B}_{IMF}$). In the dawn portion of this pass OGO-4 crossed near the expected transition from plasma sheet to polar cusp precipitation, and near 9 hrs. MLT the highly structured precipitation typical in the polar cusp is seen. In the afternoon sector a typically sharp low-latitude boundary of polar cusp electron precipitation is evident several degrees lower than typical quiescent locations. Electron flux is in units of electrons/cm^2-ster-kev-sec.

Figure 3. Three examples of high-latitude 700 ev electron precipitation on 16-17 July 1968. All three passes were at geographic local times between 8 and 12 hrs. The first pass crossed near 5 hrs. MLT, so its identification with the polar cusp is questionable.

This pass, which occurred when $\bar{B}_{IMF}$ was nearly horizontal, and the third pass, which occurred nine minutes after a southward $\bar{B}_{IMF}$ reached the earth, show low-latitude boundaries of precipitation near typical quiescent locations. The second pass, which occurred after one hour of southward $\bar{B}_{IMF}$, shows a boundary at least 7^{o} below quiescent locations. AE hourly averages and the GSM Z component of $\bar{B}_{IMF}$ are shown in the top panel. $\bar{B}_{IMF}$ was directed nearly parallel with the earth-sun line, accounting for the 15-20 min. delay times, which were deduced from polar cap and equatorial magnetograms.

Figure 4. Polar cap, equatorial and auroral zone magnetograms for times corresponding to the second and third passes of Figure 3. Arrows indicate onset times of disturbances caused by the arrival of southward $\bar{B}_{IMF}$ at the earth.

Figure 5. Locations of the lower boundary of polar cusp electron precipitation for 10 cases which followed sharp onsets of southward $\bar{B}_{IMF}$. In each case the onset of southward $\bar{B}_{IMF}$ was preceded by at least a half hour of horizontal or northward field, and occurred during quiet conditions or during the late recovery phase of a substorm. Solid curves are the results of flux conservation calculations assuming that field-line reconnection occurs between the dayside geomagnetic field and a southward interplanetary field of 0.5γ (upper curve) and 1γ (lower curve).

Figure 6. Locations of the low-latitude boundary of polar cusp electron precipitation for various geomagnetic tilt angles. All

observations occurred when $\bar{B}_{IMF}$ was northward and no substorm activity was evident in 2.5-minute AE values. Open circles are average locations of the > 35 kev electron boundary for local times 10-18 hours as reported by Feldstein and Starkov (1970). The upper dashed curve indicates the invariant latitude of the first open field line as a function of tilt-angle, as calculated from the model magnetosphere of Mead and Fairfield (1971). The lower dashed curve lies 3^{o} below the upper curve.

Figure 7. Locations of the high-latitude boundary of polar cusp electron precipitation for various tilt angles, taken from Hoffman (1971) and modified as follows: (1) Solid circles indicate cases where B_{IMF} was clearly southward and/or when a substorm was in progress, (2) Squares indicate cases with no substorm activity, but when $\bar{B}_{IMF}$ was nearly horizontal and was neither clearly northward nor southward. The original open circles have been retained for cases with no substorm activity and when $\bar{B}_{IMF}$ was clearly northward.

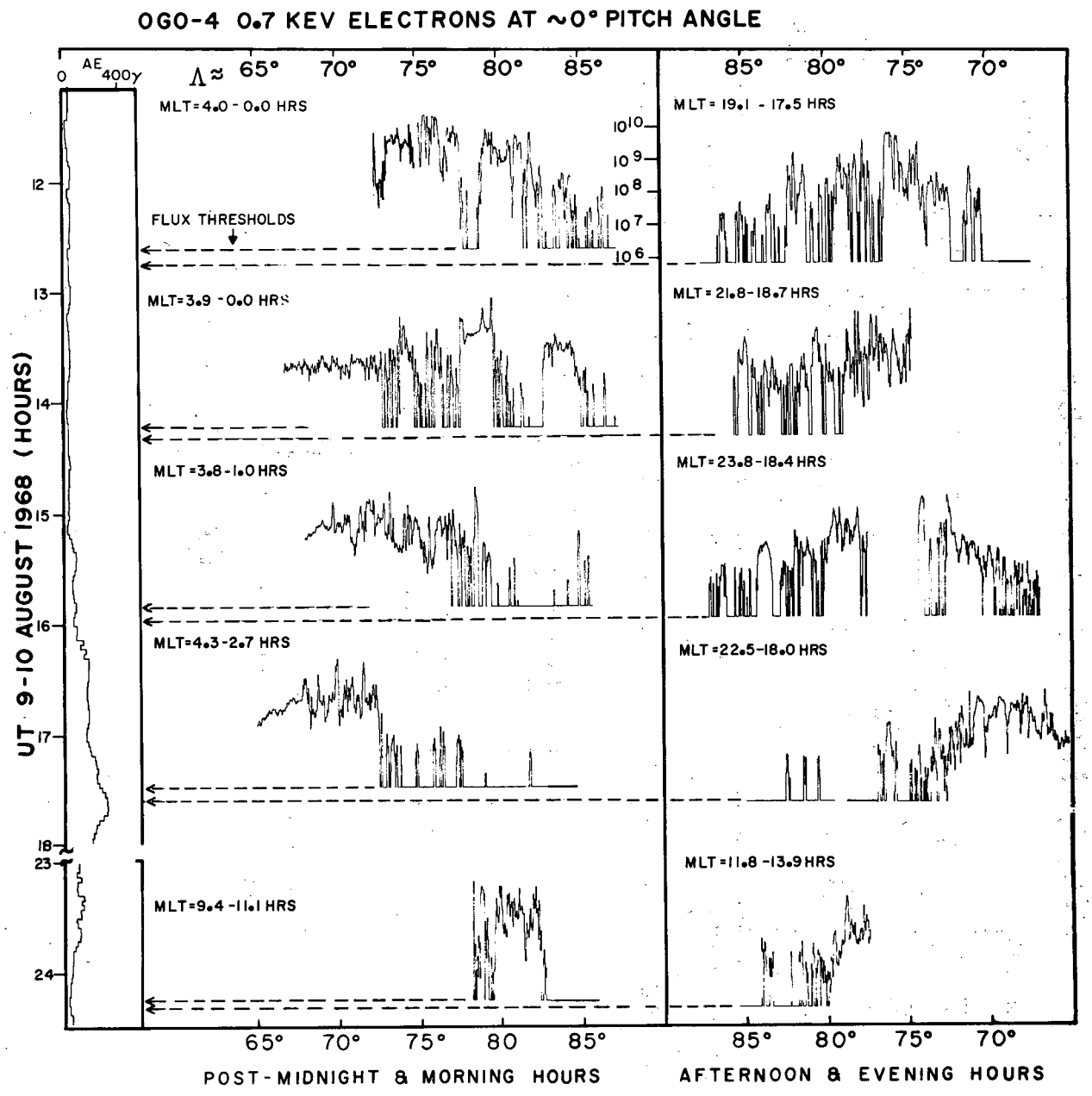
OGO-4 0.7 KEV ELECTRONS AT ~0° PITCH ANGLE
0 AE 400γ
Λ≈ 65° 70° 75° 80° 85°
85° 80° 75° 70°
MLT=4.0 - 0.0 HRS
MLT= 19.1 - 17.5 HRS
FLUX THRESHOLDS
MLT=3.9 - 0.0 HRS
MLT= 21.8-18.7 HRS
MLT=3.8-1.0 HRS
MLT=23.8-18.4 HRS
MLT=4.3-2.7 HRS
MLT=22.5-18.0 HRS
MLT=9.4 -11.1 HRS
MLT=11.8 -13.9 HRS
UT 9-10 AUGUST 1968 (HOURS)
12
13
14
15
16
17
18
23
24
POST-MIDNIGHT & MORNING HOURS
AFTERNOON & EVENING HOURS

FIGURE 1

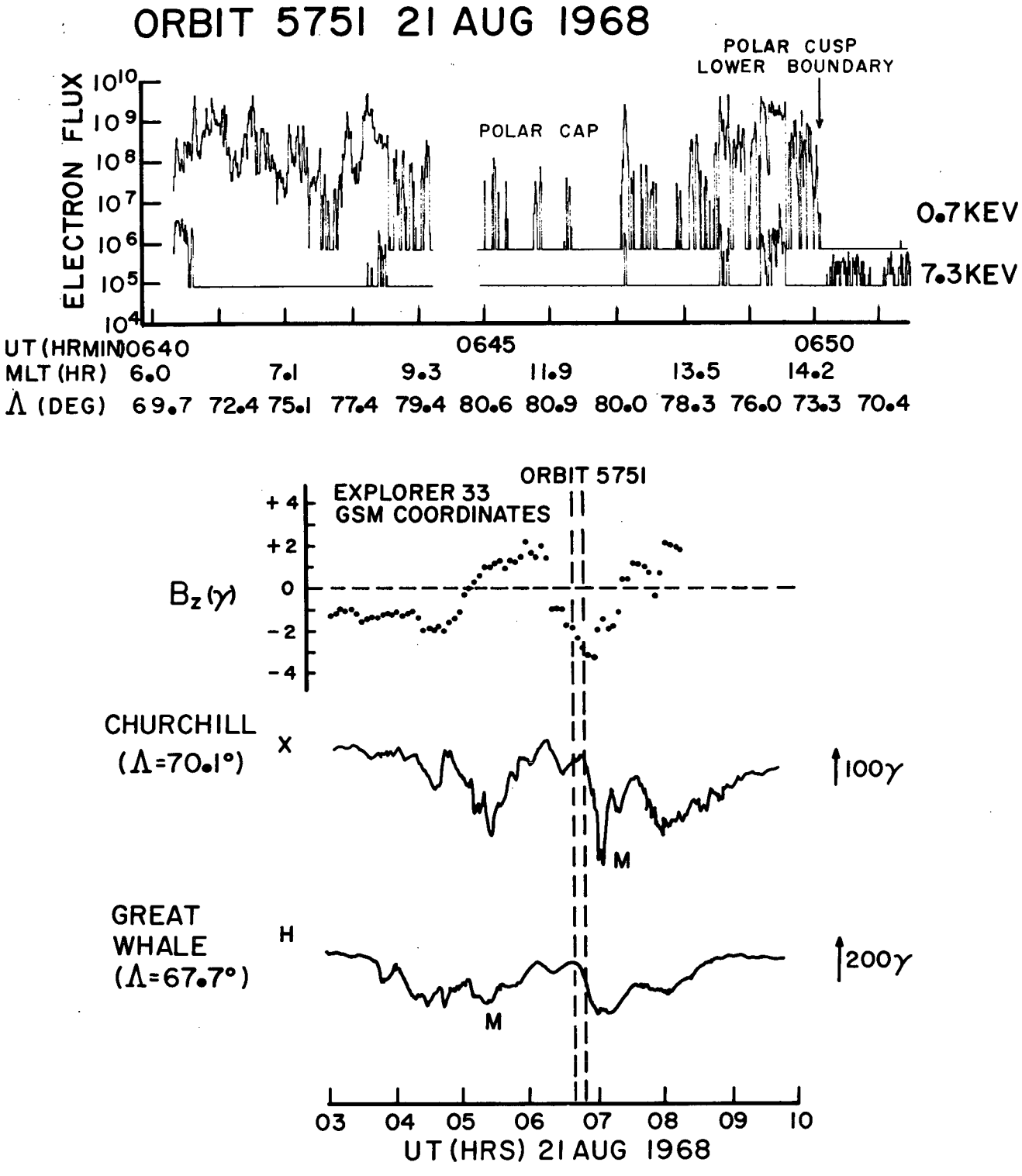
ORBIT 5751 21 AUG 1968
POLAR CUSP
LOWER BOUNDARY
POLAR CAP
ELECTRON FLUX
10^{10}
10^{9}
10^{8}
10^{7}
10^{6}
10^{5}
10^{4}
0.7KEV
7.3KEV
UT (HRMIN) 0640
0645
0650
MLT (HR) 6.0 7.1 9.3 11.9 13.5 14.2
Λ (DEG) 69.7 72.4 75.1 77.4 79.4 80.6 80.9 80.0 78.3 76.0 73.3 70.4
ORBIT 5751
EXPLORER 33
GSM COORDINATES
+4
+2
0
-2
-4
B_z (γ)
CHURCHILL
(Λ=70.1°)
X
100γ
M
GREAT
WHALE
(Λ=67.7°)
H
200γ
M
03 04 05 06 07 08 09 10
UT (HRS) 21 AUG 1968

FIGURE 2

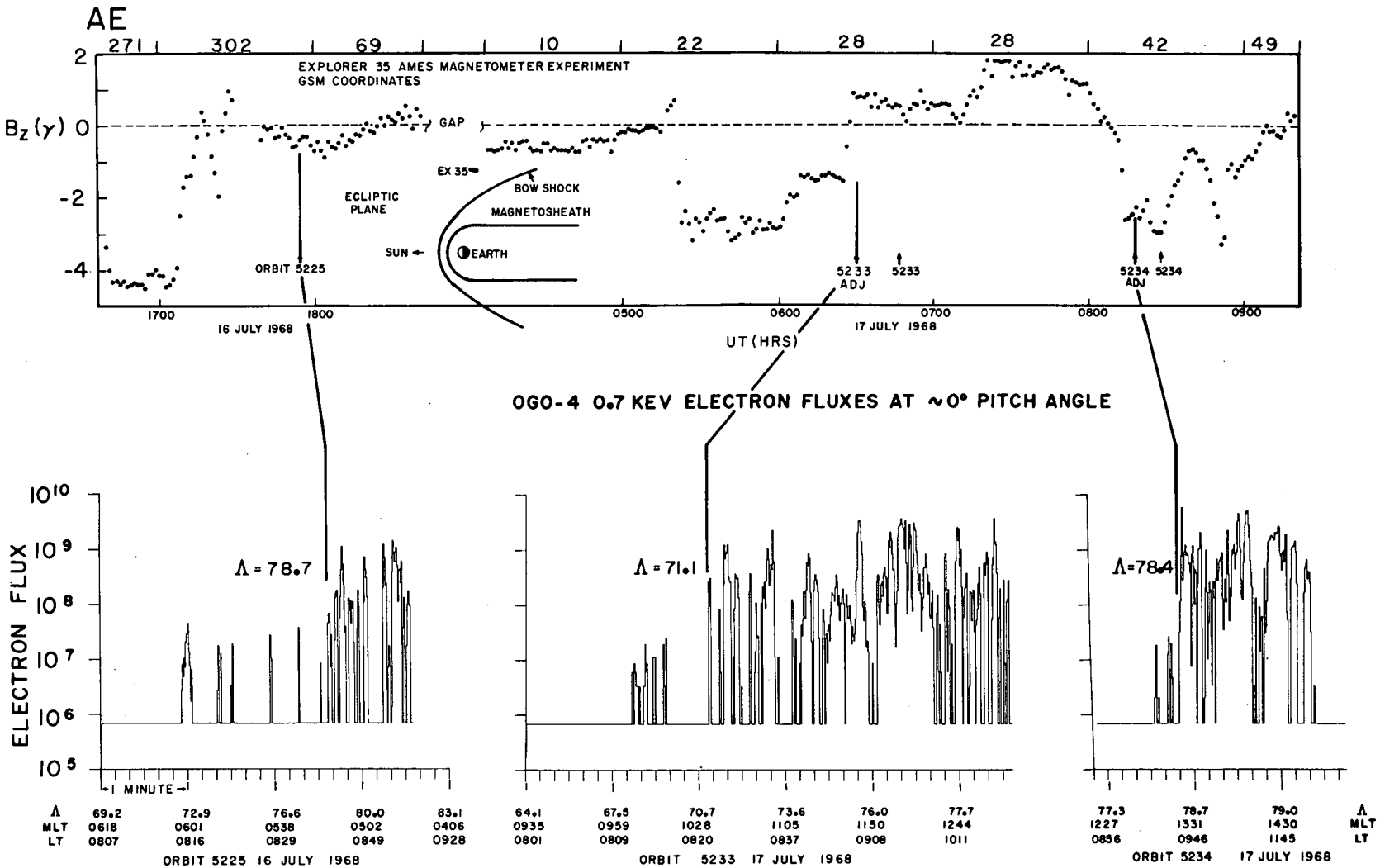
AE
271
302
69
10
22
28
28
42
49
EXPLORER 35 AMES MAGNETOMETER EXPERIMENT
GSM COORDINATES
$B_z(\gamma)$
2
0
-2
-4
GAP
EX 35
BOW SHOCK
MAGNETOSHEATH
ECLIPTIC PLANE
SUN
EARTH
ORBIT 5225
5233 ADJ
5233
5234 ADJ
5234
1700
1800
0500
0600
0700
0800
0900
16 JULY 1968
17 JULY 1968
UT (HRS)
OGO-4 0.7 KEV ELECTRON FLUXES AT ~0° PITCH ANGLE
ELECTRON FLUX
10^{10}
10^{9}
10^{8}
10^{7}
10^{6}
10^{5}
Λ = 78.7
Λ = 71.1
Λ=78.4
1 MINUTE
Λ 69.2 72.9 76.6 80.0 83.1
MLT 0618 0601 0538 0502 0406
LT 0807 0816 0829 0849 0928
ORBIT 5225 16 JULY 1968
64.1 67.5 70.7 73.6 76.0 77.7
0935 0959 1028 1105 1150 1244
0801 0809 0820 0837 0908 1011
ORBIT 5233 17 JULY 1968
77.3 78.7 79.0 Λ
1227 1331 1430 MLT
0856 0946 1145 LT
ORBIT 5234 17 JULY 1968

FIGURE 3

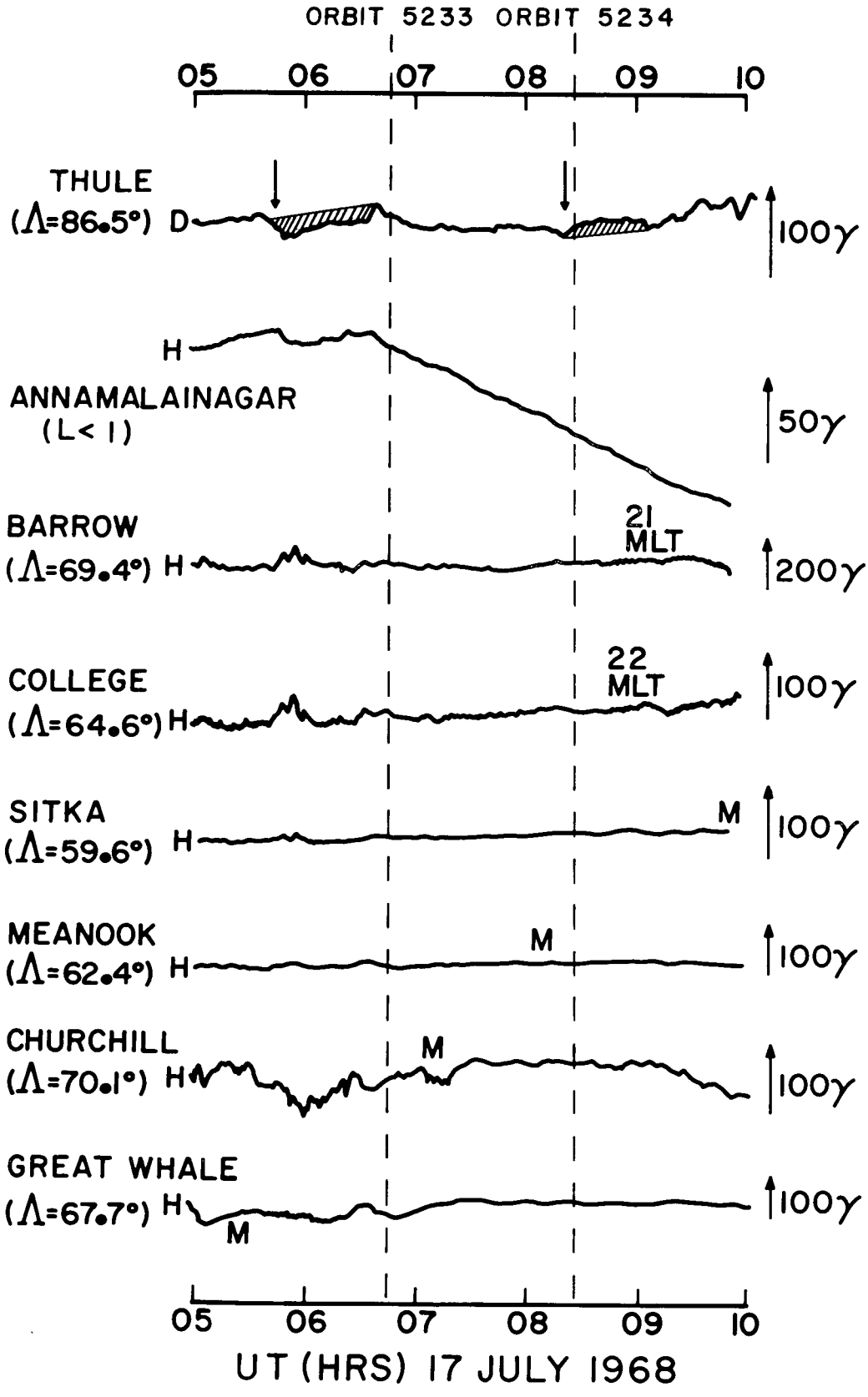
ORBIT 5233
ORBIT 5234
05
06
07
08
09
10
THULE
(Λ=86.5°)
D
100γ
H
ANNAMALAINAGAR
(L< 1)
50γ
BARROW
(Λ=69.4°)
H
21
MLT
200γ
COLLEGE
(Λ=64.6°)
H
22
MLT
100γ
SITKA
(Λ=59.6°)
H
M
100γ
MEANOOK
(Λ=62.4°)
H
M
100γ
CHURCHILL
(Λ=70.1°)
H
M
100γ
GREAT WHALE
(Λ=67.7°)
H
M
100γ
05
06
07
08
09
10
UT (HRS) 17 JULY 1968

FIGURE 4

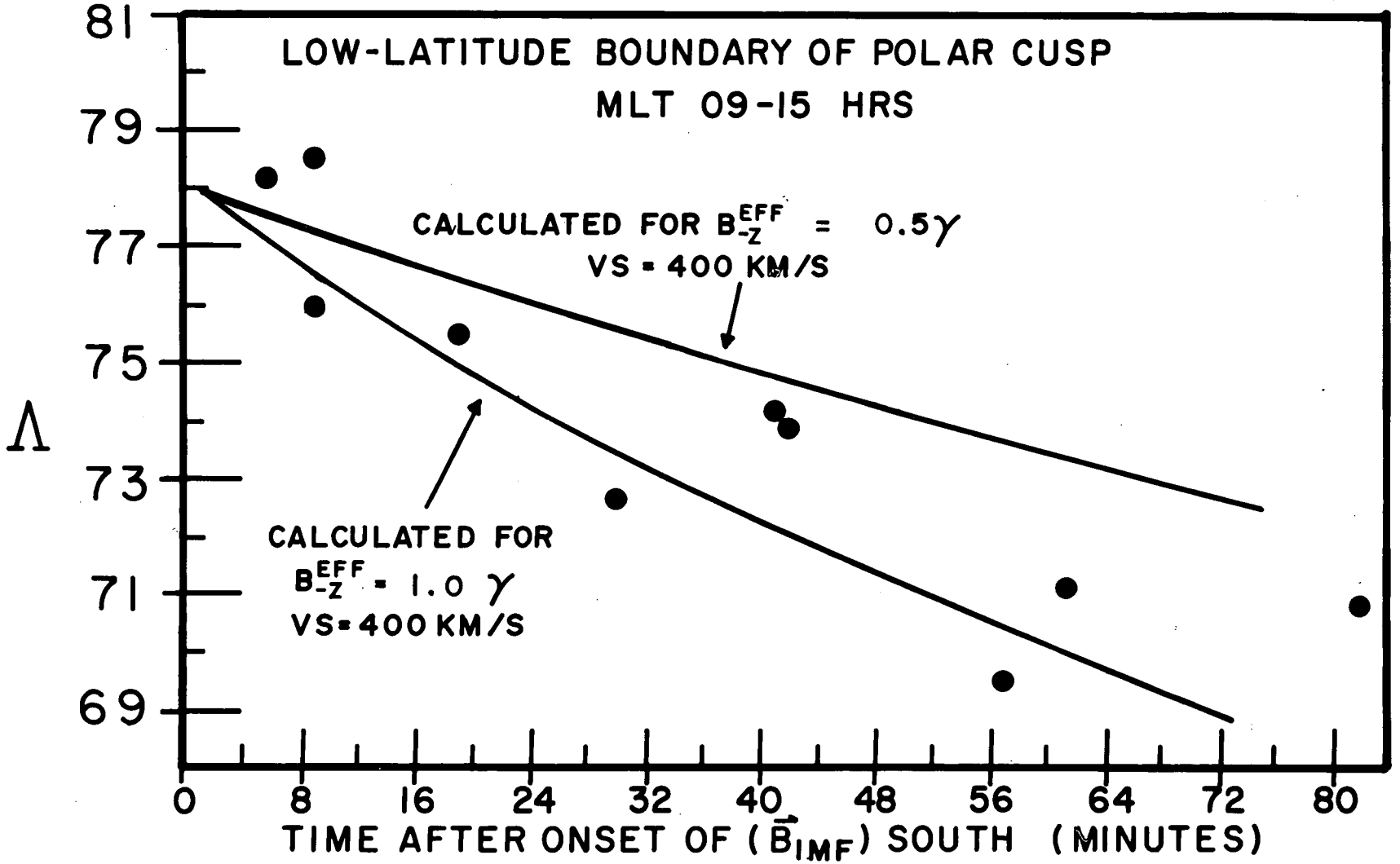
LOW-LATITUDE BOUNDARY OF POLAR CUSP
MLT 09-15 HRS
CALCULATED FOR B_{-Z}^{EFF} = 0.5γ
VS = 400 KM/S
CALCULATED FOR
B_{-Z}^{EFF} = 1.0 γ
VS = 400 KM/S
Λ
81
79
77
75
73
71
69
0
8
16
24
32
40
48
56
64
72
80
TIME AFTER ONSET OF ($\vec{B}_{IMF}$) SOUTH (MINUTES)

FIGURE 5

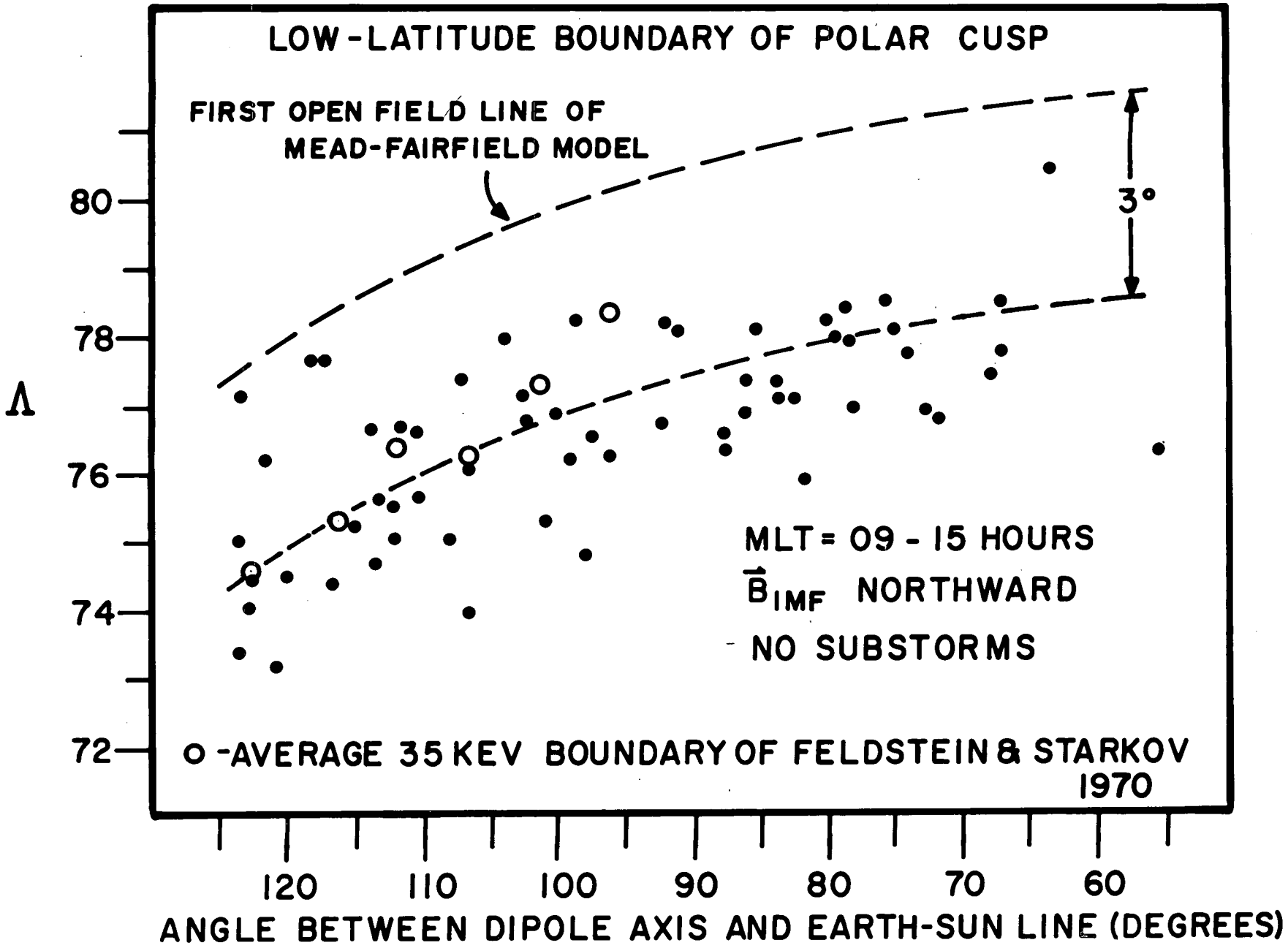
LOW-LATITUDE BOUNDARY OF POLAR CUSP
FIRST OPEN FIELD LINE OF
MEAD-FAIRFIELD MODEL
3°
80
78
76
74
72
Λ
MLT = 09 - 15 HOURS
$\vec{B}_{IMF}$ NORTHWARD
NO SUBSTORMS
O -AVERAGE 35 KEV BOUNDARY OF FELDSTEIN & STARKOV
1970
120
110
100
90
80
70
60
ANGLE BETWEEN DIPOLE AXIS AND EARTH-SUN LINE (DEGREES)

FIGURE 6

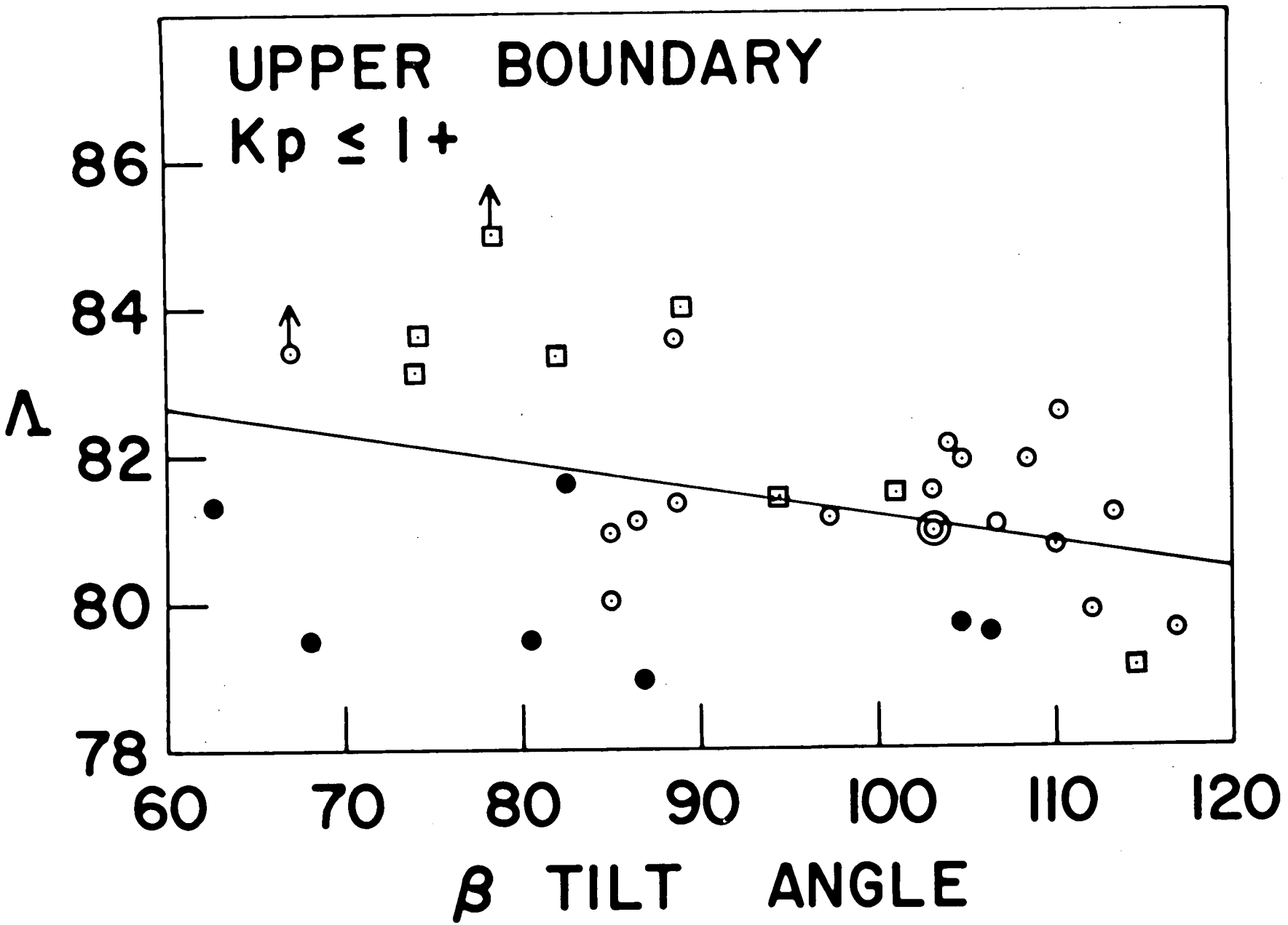
UPPER BOUNDARY
Kp ≤ 1+
86
84
82
80
78
Λ
60
70
80
90
100
110
120
β TILT ANGLE

FIGURE 7